Heteromeric Assembly of Kv2.1 with Kv9.3: Effect on the State Dependence of Inactivation

Daniel Kerschensteiner and Martin Stocker
Molekulare Biologie Neuronaler Signale, Max-Planck-Institut für Experimentelle Medizin, D-37075 Göttingen, Germany

ABSTRACT Modulatory α-subunits of Kv channels remain electrically silent after homomeric expression. Their interactions with Kv2 α-subunits via the amino-terminal domain promote the assembly of heteromeric functional channels. The kinetic features of these heteromers differ from those of Kv2 homomers, suggesting a distinct role in electrical signaling. This study investigates biophysical properties of channels emerging from the coexpression of Kv2.1 with the modulatory α-subunit Kv9.3. Changes relative to homomeric Kv2.1 concern activation, deactivation, inactivation, and recovery from inactivation. A detailed description of Kv2.1/Kv9.3 inactivation is presented. Kv2.1/Kv9.3 heteromers inactivate in a fast and complete fashion from intermediate closed states, but in a slow and incomplete manner from open states. Intermediate closed states of channel gating can be approached through partial activation or deactivation, according to a proposed qualitative model. These transitions are rate-limiting for Kv2.1/Kv9.3 inactivation. Finally, based on the kinetic description, we propose a putative function for Kv2.1/Kv9.3 heteromers in rat heart.

INTRODUCTION

Potassium channels form the most diverse class in the ion channel superfamily, giving rise to a large variety of currents, the kinetics of which are shaped to the requirements of their physiological function (Hille, 1992). Part of this diversity is of combinatorial origin, inasmuch as potassium channels are oligomeric protein complexes (MacKinnon, 1991; Parcej et al., 1992). Participation of different proteins occurs by two mechanisms. Either distinct α-subunits assemble into heterotetrameric channels with all subunits lining the pore (Christie et al., 1990; Isacoff et al., 1990; Ruppersberg et al., 1990), or auxiliary β-subunits associate with tetrameric channel complexes, changing their kinetic properties (Rettig et al., 1994). Modulatory α-subunits form a group of proteins that contributes to the diversity of potassium channels by the first mechanism. So far, this group includes Kv5.1, Kv6.1 (Drewe et al., 1992), Kv8.1(Kv2.3r) (Hugnot et al., 1996; Castellano et al., 1997), and Kv9.1–9.3 (Patel et al., 1997; Salinas et al., 1997b; Stocker and Kerschensteiner, 1998). These α-subunits are highly similar to other Kv α-subunits by primary sequence, yet they are unable to form homomeric conducting channels in heterologous expression systems (Drewe et al., 1992; Hugnot et al., 1996; Salinas et al., 1997b; Stocker and Kerschensteiner, 1998). Specific N-terminal interactions between Kv2- and modulatory α-subunits promote the assembly of heterotetrameric channels (Post et al., 1996; Kramer et al., 1998; Stocker et al., 1999) displaying altered characteristics in comparison to homomeric Kv2 channels (Hugnot et al., 1996; Post et al., 1996; Castellano et al., 1997; Kramer et al., 1998).

The Kv2 subfamily is known to participate in the formation of channels underlying delayed rectifier currents (Frech et al., 1989; Hwang et al., 1992; Tsunoda and Salkoff, 1995). Expressed in large variety of excitable cells, this family is thought to be involved in the repolarization of different types of action potentials (Quattrocki et al., 1994; Barry et al., 1995; Tsunoda and Salkoff, 1995). There was some incongruity between the diverse kinetic requirements and the fact that the Kv2 subfamily contains only two members, Kv2.1 and Kv2.2, with very similar kinetic characteristics (Frech et al., 1989; Van Dongen et al., 1990; Hwang et al., 1992). Furthermore, differences between the regional and developmental expression of Kv2 subunits and the respective patterns of the putatively mediated currents suggest the involvement of further subunits in the formation of native channels (Barry et al., 1995; Xu et al., 1996). In this context, the finding that Kv2 subunits are the predominant targets for an increasing number of modulatory α-subunits might help to resolve previous discrepancies.

The comparative study of heteromeric Kv2.1/Kv9.3 and homomeric Kv2.1 presented here shows that coexpression of Kv2.1 and Kv9.3 subunits results in channels with unique biophysical properties. Particular emphasis is placed on their inactivation. In agreement with the work of Klemic et al. (1998), we show that Kv2.1 inactivates from both open and intermediate closed states. In contrast, Kv2.1/Kv9.3 does not inactivate from open states, but in a fast and complete manner from intermediate closed states. This results in a U-shaped steady-state inactivation curve of Kv2.1/Kv9.3. Furthermore, we demonstrate that the rate-limiting steps in this inactivation are transitions usually occurring during activation and deactivation. Finally, as predicted for a channel with an accelerated closed-state inactivation and recovery, the maximum of cumulative inactivation is shifted toward higher frequencies. The observed kinetic behavior

Received for publication 11 January 1999 in final form 13 April 1999.

Address reprint requests to Dr. Martin Stocker, Abteilung Molekulare Biologie Neuronaler Signale, Max-Planck Institut für Experimentelle Medizin, Hermann-Rein-Strasse 3, D-37075 Göttingen, Germany. Tel.: +49-551-3899-618;Fax:+49-551-3899-644;E-mail:stocker@mail.mpiem.gwdg.de.

0006-3495/99/07/248/10 $2.00

suggests a new possible role for Kv2.1/Kv9.3 in the regulation of electrical signals.

MATERIALS AND METHODS

Plasmids, cDNAs, cRNA synthesis, and expression in *Xenopus* oocytes

The cDNA clone of Kv2.1 (DRK1) was kindly provided by Dr. R. Joho. To generate full-length Kv2.1, four amino acids (MPAG) were introduced in frame by oligonucleotide-aided gene assembly at the amino-terminal end of Kv2.1. Subsequently, the full-length clone was assembled in the oocyte expression vector superGEM. The coding region of Kv9.3 was cloned into the transcription vector psGEM (Stocker and Kerschensteiner, 1998). Capped cRNAs were synthesized in vitro after linearization of the plasmids and transcription with T7 RNA polymerase (Krieg and Melton, 1987). Isolation of oocytes (stage V–VI) from *Xenopus laevis* and cRNA injection were performed as described previously (Stühmer, 1992). Kv2.1 currents were recorded from oocytes injected with 12.5 pg cRNA. For coexpression experiments, 25 pg of Kv2.1 cRNA and 125 pg of Kv9.3 cRNA were injected per oocyte.

Electrophysiological characterization

Whole-cell currents were recorded 1–4 days after injection under two-electrode voltage-clamp control, using a Turbo TEC-10CD amplifier (NPI-Elektronik, Tamm, Germany). Intracellular electrodes had resistances of 0.4–0.8 MΩ when filled with 2 M KCl. Leak and capacitive currents were subtracted on-line using a *P*/*n* protocol, except for pulses evoking cumulative inactivation. Currents were low-pass filtered at 0.7–1 kHz (−3 dB) and sampled at 3–5 kHz. The standard bath solution constantly perfused was normal frog Ringer (NFR) containing (in mM) 115 NaCl, 2.5 KCl, 1.8 $CaCl_2$, 10 HEPES-NaOH (pH 7.2). In experiments in which KCl concentrations were raised, NaCl concentrations were lowered accordingly, so that the sum of KCl and NaCl remained constant. To prevent influences of elevated extracellular potassium concentrations on channel gating, the recordings for deactivation were performed in NFR. All experiments were carried out at room temperature (20–22°C). Data acquisition and analysis were performed with the Pulse+PulseFit software package (HEKA Elektronik, Lambrecht, Germany), EXCEL (Microsoft), and IGOR (Wavemetrics). Boltzman functions of the type $P_o/P_{o,max}$ or I/I_{max} = offset + $1/(1 + \exp((V_{1/2} - V_m/a))$ were used to fit activation and inactivation, respectively.

Statistical analysis

Data are given as mean ± SE, with *n* specifying the number of independent experiments. Statistical significance was evaluated using a two-tailed Student's *t*-test ($p \leq 0.05$).

RESULTS

Differences of activation and deactivation between heteromeric Kv2.1/Kv9.3 and homomeric Kv2.1 channels

Kv9.3, a member of the Kv9 subfamily, is known to interact via the T1-domain with the Kv2.1 protein (Stocker et al., 1999). Coinjection of high amounts of Kv9.3 cRNA in *Xenopus* oocytes suppresses currents mediated by Kv2.1 α-subunits (Stocker et al., 1999). In this study we characterize the functional heteromeric channels resulting from the coinjection of lower amounts of Kv9.3 cRNA with Kv2.1.

To test the voltage dependence of activation, currents were elicited by voltage steps from a holding potential of −90 mV to depolarized potentials (increment: 10 mV), followed by a constant hyperpolarization to −40 mV (Fig. 1 *A*). The initial current in the hyperpolarized segment was used to determine the voltage dependence of the steady-state open probability for heteromeric Kv2.1/Kv9.3 and homomeric Kv2.1 channels. The normalized open probability ($P_o/P_{o,max}$)-voltage curve of Kv2.1/Kv9.3 channels was displaced toward hyperpolarized potentials compared to Kv2.1 channels, without major changes in the slope (a_n) (Fig. 1 *A* and Table 1).

To investigate the kinetics of activation, 200-ms pulses to increasing potentials were delivered (*scaled traces at +20 mV*, Fig. 1 *B*). For depolarizations below +10 mV, the rising phase of both currents could be described by monoexponential functions, and the calculated time constants were indistinguishable (Fig. 1 *C* and Table 1). At positive potentials two time constants were required to adequately fit the Kv2.1/Kv9.3 current. The fast component remained indistinguishable from the time constant calculated for Kv2.1 currents at all potentials, whereas the slower component displayed similar voltage dependence, but was five- to sevenfold slower (Table 1). Along with this slowing of activation kinetics, closure of channels was found to be five to seven times slower for Kv2.1/Kv9.3 when compared to Kv2.1 (Fig. 1, *D* and *E*). Unlike activation, deactivation was sufficiently matched by a monoexponential fit for both channel types over the entire voltage range tested (Table 1). Furthermore, the voltage dependence of deactivation of Kv2.1/Kv9.3 was increased (Kv2.1/Kv9.3, 14 mV/*e*-fold increase; Kv2.1, 20 mV/*e*-fold increase) (Fig. 1 *E*). Channel activation and deactivation are thought to require the participation of all pore-forming subunits for their completion. Thus the observed changes in the kinetics and voltage dependence of heteromeric Kv2.1/Kv9.3 channels suggest that Kv9.3 comprises part of this gating apparatus.

Differences in state dependence of inactivation of Kv2.1/Kv9.3 and Kv2.1

In a recently proposed kinetic model, inactivation of Kv2.1 has been separated into two distinct processes: inactivation from open and from closed states (Klemic et al., 1998). We started to analyze whether the state dependence of inactivation for Kv2.1/Kv9.3 is changed with respect to Kv2.1 by measuring inactivation from the open state. Oocytes were depolarized for 10 s to a voltage where the initial open probability is at maximum (+40 mV), and the observed current decay was fitted with a monoexponential function (Fig. 2 *A*). At the end of the pulse 84% of the Kv2.1/Kv9.3 current and 20% of the Kv2.1 current remained (Table 1), indicating that for the heteromeric channel little inactivation occurs from the open state or states linked to it through voltage-independent transitions. For Kv2.1 and Kv2.1/Kv9.3 inactivation was voltage-independent in the range of

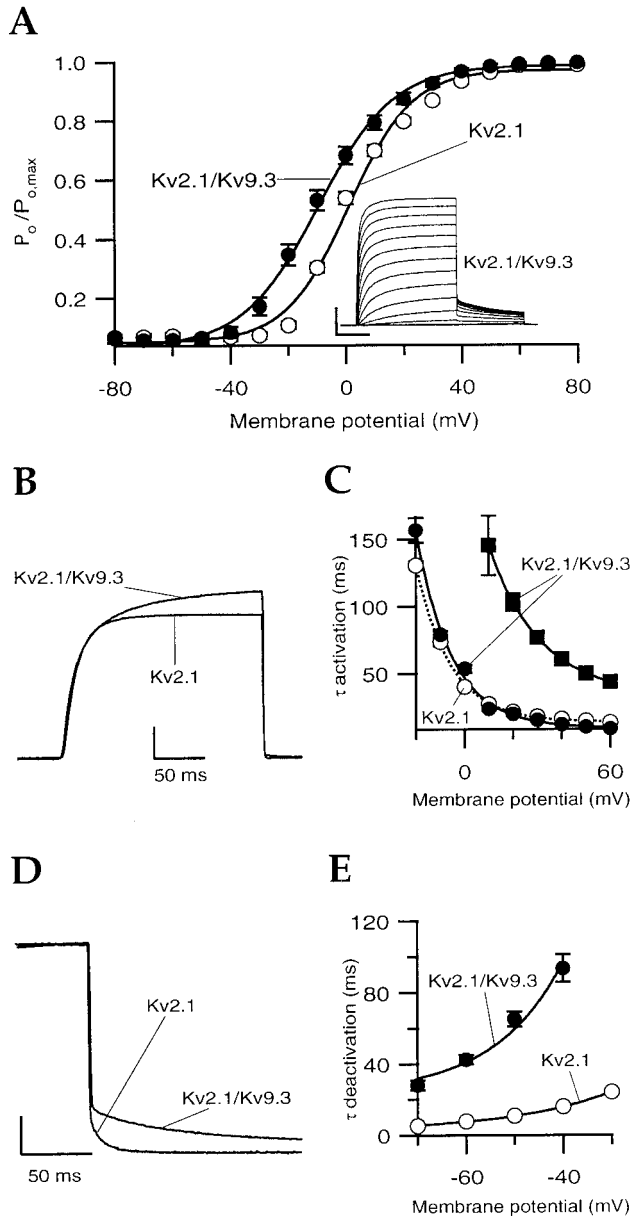

FIGURE 1 Comparison of activation and deactivation of homomeric Kv2.1 and heteromeric Kv2.1/Kv9.3 channels. The holding potential was −90 mV in all pulses. (*A*) To determine steady-state activation, conditioning pulses from −80 to +80 mV (increment: 10 mV) were applied, lasting 200 ms for Kv2.1 and 300 ms for Kv2.1/Kv9.3 to account for differences in activation kinetics. Subsequently, voltage was clamped to −40 mV, and the initial current in this segment was estimated from a monoexponential fit to its decay. The relative open probabilities derived from the initial currents were plotted against the voltages of the depolarizing step and fitted with a Boltzmann function ($n = 6–8$). *Inset*: Kv2.1/Kv9.3 currents elicited by the above protocol. Scale bars: horizontal, 100 ms; vertical, 8 μA. (*B*) Scaled and superimposed current traces of Kv2.1 and Kv2.1/Kv9.3 elicited by depolarizations to +20 mV. Vertical scale bar: Kv2.1, 2.35 μA; Kv2.1/Kv9.3, 2 μA. (*C*) Time constants (τ) of activation obtained from mono- or double-exponential fits to current traces evoked by 200-ms pulses were plotted as a function of test potentials. Double-exponential functions were necessary to fit the activation of Kv2.1/Kv9.3 at positive membrane potentials ($n = 6$). (*D*) Deactivation of Kv2.1 and Kv2.1/Kv9.3, shown as scaled and superimposed current traces, stepping from +40 to −50 mV. Vertical scale bar: Kv2.1, 2.7 μA; Kv2.1/Kv9.3, 1.7 μA. (*E*) Time constant (τ) of deactivation plotted as a function of test potentials. After a conditioning pulse ensuring maximum channel opening (+40 mV, Kv2.1: 200 ms; Kv2.1/Kv9.3: 300 ms), the voltage was stepped to various potentials. The observed current relaxation was fitted with a monoexponential function, and τ values were calculated ($n = 6$).

TABLE 1 Kinetic parameters of Kv2.1/Kv9.3 and Kv2.1

Parameter	Kv2.1/Kv9.3	Kv2.1
$V_{n,1/2}$ (mV)	−9.5 ± 2	1 ± 1
a_n (mV)	13 ± 0.5	11 ± 0.5
τ_{act} (ms) (at −10 mV)	79 ± 2	74 ± 3
$\tau_{1,act}$ (ms) (at +20 mV)	20 ± 1	21 ± 1
$\tau_{2,act}$ (ms) (at +20 mV)	103 ± 6	—
τ_{deact} (ms) (at −50 mV)	65 ± 4	11 ± 0.5
$V_{h,1/2}$ (mV)	−54.8 ± 1.8	−34.7 ± 0.6
a_h (mV)	−6.6 ± 0.8	−4.4 ± 0.1
Inact. (%)* (at +40 mV)	16.2 ± 1.8	80.7 ± 2.2
$\tau_{recovery}$ (ms) (at −130 mV)	124 ± 4	131 ± 6
$\tau_{recovery}$ (ms) (at −80 mV)	335 ± 21	1308 ± 141

Kinetic parameters for activation ($V_{n,1/2}$; a_n) and inactivation ($V_{h,1/2}$; a_h) were obtained from fits to the respective Boltzman functions (see Materials and Methods). Time constants for activation, deactivation, and recovery for the indicated potentials were obtained by fitting mono- or double-exponentials, as indicated in the text.

*The percentage of current that is inactivated at the end of a 10-s pulse to +40 mV ($n = 6–9$).

maximum open probability (> +40 mV; data not shown), arguing that the inactivation of both channels is primarily state-dependent.

Multiple voltage-dependent conformational changes are required before channel opening (Hille, 1992). We named the states between the most deactivated state (C), which has undergone none of these changes, and the open state (O) intermediate closed states (C_i). The pulse protocol shown in Fig. 2 *B* was used to measure inactivation proceeding from nonconducting intermediate closed states. A 200-ms voltage step to +40 mV was delivered to activate channels maximally (P1), followed by a conditioning pulse of variable length (P2) to potentials below activation threshold, where channels are predicted to occupy intermediate closed states (−50 to −20 mV), and a brief voltage step (P3) identical in strength and duration to P1. At the end of P1 most channels are open, and entering the P2 segment they start to deactivate, occupying intermediate closed states from which inactivation might take place. The currents evoked by P3, consequently, represent the fraction of channels that did not inactivate during P2. Fig. 2 *B* shows the time dependence of inactivation from intermediate closed states, plotting the ratio of the currents (I_{P3}/I_{P1}) against the duration of P2. For a comparison of the two channel types, the voltages −30 mV for Kv2.1 and −40 mV for Kv2.1/Kv9.3 were used, accounting for the 10-mV difference in the steady-state activation (Fig. 1 *A*). The relative currents were fit with either monoexponential (Kv2.1: $\tau = 18.5 \pm 2.4$ s) or double-exponential (Kv2.1/Kv9.3: $\tau_{fast} = 0.63 \pm 0.09$ s and $\tau_{slow} = 3.1 \pm 0.4$ s) decay functions. Both time constants of Kv2.1/Kv9.3 compared to the single time constant for

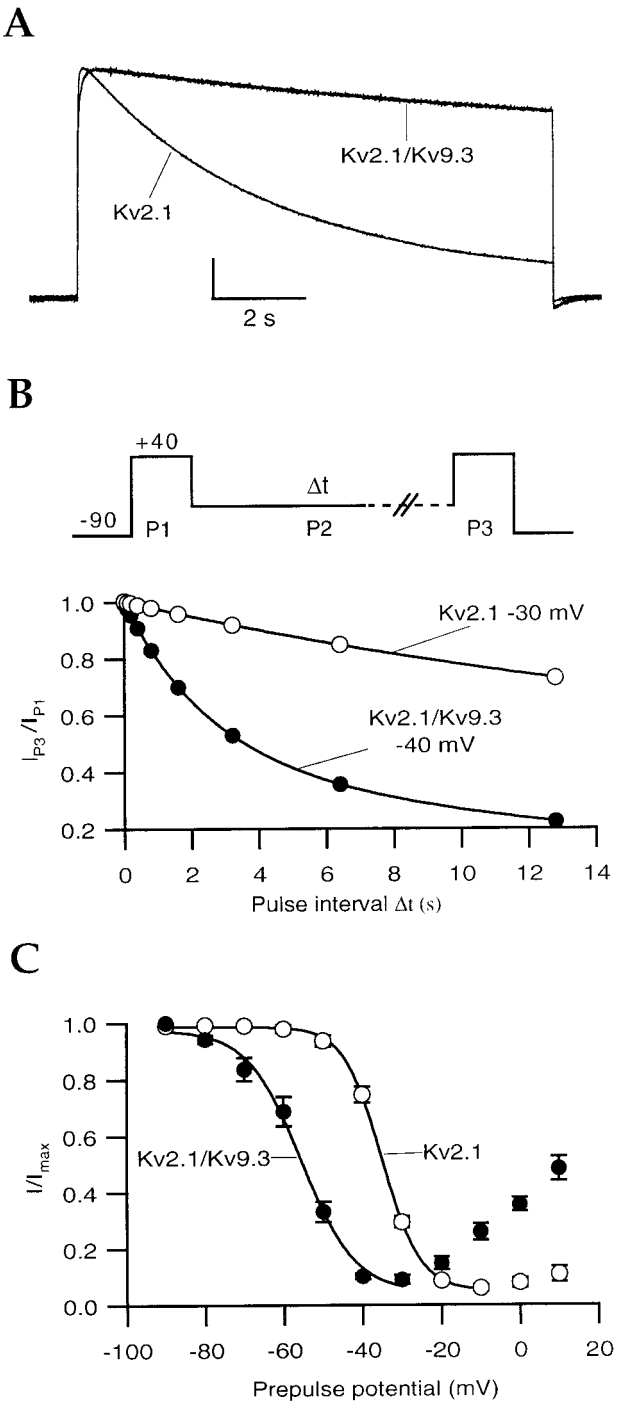

FIGURE 2 Comparison of inactivation of Kv2.1 and Kv2.1/Kv9.3. (*A*) Representative scaled and superimposed current traces of Kv2.1 and Kv2.1/Kv9.3 evoked by a 10-s test pulse from −90 to +40 mV, presenting open state inactivation. Vertical scale bar: Kv2.1, 3 μA; Kv2.1/Kv9.3, 1.8 μA. (*B*) Inactivation from intermediate closed states plotted as the ratio of peak currents (I_{P3}/I_{P1}) within a 200-ms test pulse to +40 mV in P1 and P3 against the time spent in the intervening voltage segment (P2, Kv2.1: −30 mV; Kv2.1/Kv9.3: −40 mV). Data points were fitted with monoexponential (Kv2.1) or double-exponential (Kv2.1/Kv9.3) functions. (*C*) Voltage dependence of steady-state inactivation. After 60-s prepulses ranging from −90 to +10 mV, applied in 10-mV increments, noninactivated current was determined by pulsing to +40 mV. Normalized currents were plotted against prepulse potentials and fitted with a Boltzman function to the minimum of the curve ($n = 5$).

Kv2.1 accounted for an accelerated inactivation from intermediate closed state for heteromeric channels. Currents elicited by the prepulse (P1) of consecutive pulses were compared to control for accumulation of inactivation between sweeps.

Channels showing a pronounced inactivation from intermediate closed states and little or no inactivation from the open state, like Kv2.1/Kv9.3, are predicted to present a U-shaped voltage dependence of the steady-state inactivation curve. The steady-state inactivation behaviors of Kv2.1 and Kv2.1/Kv9.3 were measured using a two-pulse protocol consisting of a conditioning prepulse of 60 s to voltages ranging from −90 to +10 mV, followed by a test pulse to +40 mV. Normalized currents evoked by the test pulse plotted against the prepulse potential revealed a slight U-shaped steady-state voltage dependence of inactivation for Kv2.1 and a more pronounced one for Kv2.1/Kv9.3 (Fig. 2 *C*). The Boltzmann functions fit down to the minimum of the U-shaped relation, which is below the activation threshold of the respective channels, primarily describe closed state inactivation. The estimated half-maximum inactivation ($V_{h,1/2}$) showed a 20-mV hyperpolarizing shift for Kv2.1/Kv9.3 compared with Kv2.1. Furthermore, the slope (a_h) was increased slightly for Kv2.1/Kv9.3 (Table 1).

Rate-limiting transitions in Kv2.1/Kv9.3 inactivation

Assuming a simplified kinetic model (Fig. 3 *A*) for the state-dependent inactivation of Kv2.1/Kv9.3, where unlike for Kv2.1 open state inactivation ($O \rightarrow I_o$) is insignificant, either reaching the state favoring inactivation (C_i) through partial activation ($C \rightarrow C_i$) or deactivation ($O \rightarrow C_i$), or the transition from there to the inactivated state ($C_i \rightarrow I_{Ci}$), could be rate-limiting. Because activation is accelerated by depolarization and deactivation is accelerated by hyperpolarization, one would assume that, if these transitions were rate-limiting, the voltage dependence of the time constants of inactivation would be opposed, depending on whether the intermediate closed states (C_i) are approached from an open state (O) or a completely deactivated state (C). To test this hypothesis, the two pulse protocols shown in the inset of Fig. 3 *B* were applied. For the pulse protocol named "activation," channels were maximally activated by stepping to +40 mV (P1), followed by a 10-s pulse to −90 mV, ensuring complete deactivation (C). Pulsing afterward to intermediate potentials (P2), ranging from −50 to −30 mV for Kv2.1/Kv9.3 and from −30 to −10 mV for Kv2.1, resulted in partial activation of the channels and subsequent inactivation after the ($C \rightarrow C_i$) transitions. The fraction of channels that did not inactivate during (P2) were measured by performing a voltage step to +40 mV (P3). The pulse protocol named "deactivation" was identical to the one used in Fig. 2 *B*. After maximum activation of the channels (P1), inactivation was evoked, after partial deactivation at P2. For both protocols the ratio of currents (I_{P3}/I_{P1}) was plotted

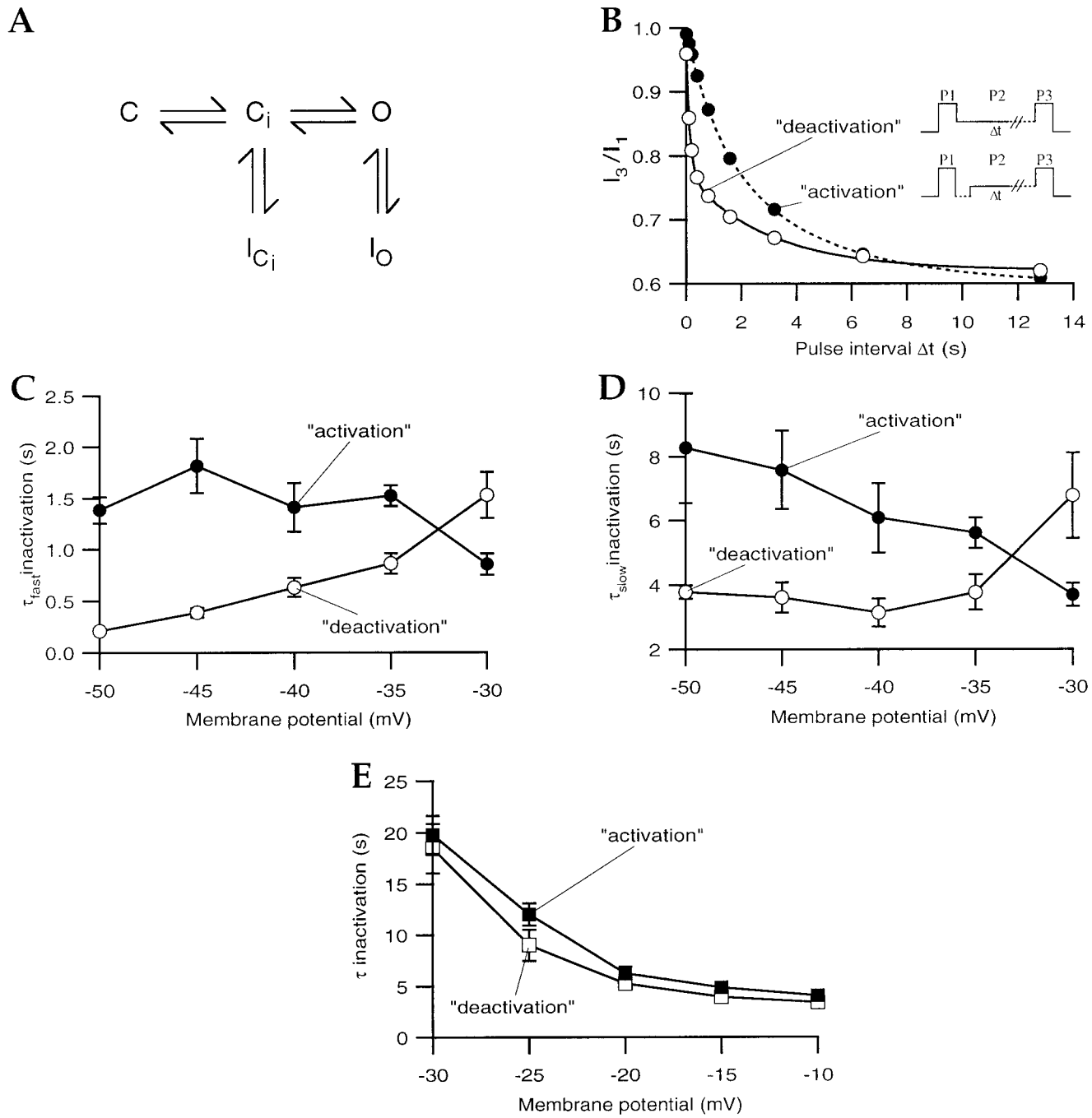

FIGURE 3 Rate-limiting steps in inactivation of Kv2.1/Kv9.3. (*A*) Simplified kinetic model for describing the inactivation of Kv2.1 and Kv2.1/9.3. O signifies open channels, C complete deactivation from which inactivation is unlikely, and C_i intermediate closed states favoring inactivation. Inactivated states reached from intermediate closed states are termed I_{Ci}, and inactivated states reached by open channels are called I_o. Both inactivations are primarily voltage-independent, whereas transitions between C, C_i, and O are considered voltage-dependent. (*B*) Representative examples of the time course of intermediate closed state inactivation (P2: −45 mV) for heteromeric Kv2.1/Kv9.3 channels. At −45 mV the time dependence of inactivation was measured with the pulse protocols shown in the inset and named "activation" and "deactivation." The names denote the different routes along which intermediate closed states were reached. The pulse protocol "deactivation" is described in Fig. 2 *B*, whereas to measure the time dependence of inactivation starting from completely deactivated channels ("activation"), oocytes were clamped for 10 s to −90 mV after P1 (see *inset*). Data points were fitted with double-exponential functions. In *C*, *D*, and *E*, time constants (τ) describing the time dependence of inactivation estimated from measurements shown in *B* were plotted against the voltage of the intervening segment (P2) for Kv2.1/Kv9.3 (*C, D*) and Kv2.1 (*E*). Voltages at P2 ranging from −30 to −50 mV for Kv2.1/Kv9.3 and −10 to −30 mV for Kv2.1 were varied in increments of 5 mV. For each voltage, five to eight experiments were performed.

against the increasing durations of the pulse P2 to monitor the time dependence of inactivation (Fig. 2 *B*). For Kv2.1/Kv9.3, this time dependence was best described by a double-exponential fit. Furthermore, the voltage dependence of the fast and slow time constants was estimated by stepping to different voltages in P2 (Fig. 3, *C* and *D*). For Kv2.1/

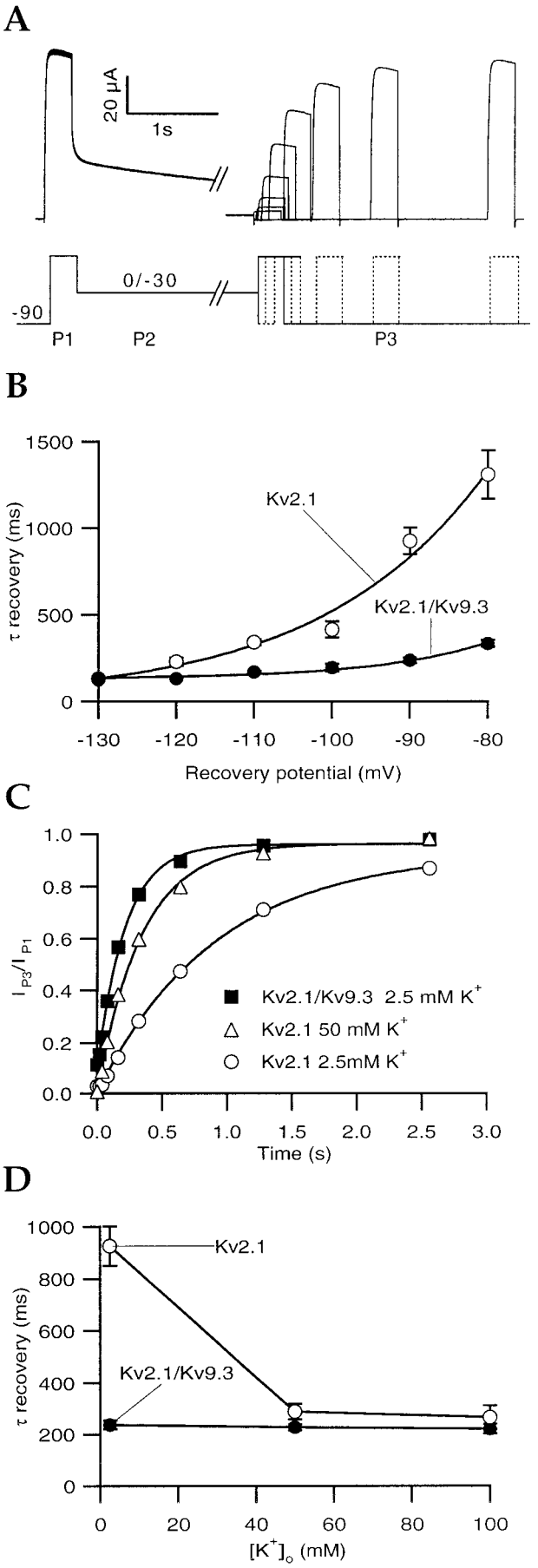

Kv9.3, both time constants gave results that were qualitatively the same. Inactivation along the $C \rightarrow C_i$ transitions ("activation") was accelerated with increasing depolarization, whereas inactivation after the $O \rightarrow C_i$ transitions ("deactivation") was accelerated by hyperpolarization. This indicates that reaching C_i is the rate-limiting step for inactivation of heteromeric Kv2.1/Kv9.3 channels. Using either the "activation" or the "deactivation" pulse protocol for Kv2.1 gave parallel curves for the voltage dependence of inactivation (Fig. 3 *E*). This is likely to be explained by inactivation occurring similarly from intermediate closed states on one hand, or the open state and those states linked to it by voltage-independent transitions on the other hand.

Recovery from inactivation of Kv2.1/Kv9.3 is accelerated and displays reduced voltage dependence and potassium sensitivity

Because the coexpression of the modulatory α-subunit Kv9.3 had a pronounced effect on the inactivation of Kv2.1, we investigated whether the recovery from inactivation was also altered. Recovery from inactivation was measured with the pulse protocol shown in Fig. 4 *A*. A short pulse to +40 mV (P1) determined the maximally available current and was followed by a conditioning pulse of 30 s to −30 mV for Kv2.1/Kv9.3 and 10 s to 0 mV for Kv2.1 to induce inactivation. The voltages of the conditioning pulse were near the respective minimum of the U-shaped relation for the voltage dependence of inactivation (Fig. 2 *C*). Inactivated channels were allowed to recover for varying intervals at potentials ranging from −130 to −80 mV before a short test pulse (P3) to +40 mV was given. Fig. 4 *A* shows a representative trace of the recovery from inactivation for Kv2.1 at −100 mV. The time course of recovery from inactivation was obtained by plotting the fraction of the recovered current (I_{P3}/I_{P1}) against the time spent at the recovery potential and

FIGURE 4 Comparing voltage and potassium dependence of recovery from inactivation for Kv2.1/Kv9.3 and Kv2.1. (*A*) Simplified scheme of the pulse protocol used to measure recovery from inactivation. After a pulse to +40 mV (P1), channels were inactivated by a conditioning pulse (P2; Kv2.1: 10 s, 0 mV; Kv2.1/Kv9.3: 30 s, −30 mV). At these voltages inactivation was nearly at maximum for both channels (Fig. 2 *B*). Subsequently, recovery was measured after increasing intervals at various potentials. Representative current traces show the recovery from inactivation (recovery potential: −100 mV) after complete inactivation of Kv2.1 (only part of the conditioning pulse is shown). (*B*) The time constants of recovery from inactivation for Kv2.1 and Kv2.1/Kv9.3 were plotted versus different recovery potentials tested. Time constants were derived from monoexponential fits to normalized currents (I_{P3}/I_{P1}) from measurements like the one shown in *A* ($n = 5$). (*C*) The time course of recovery from inactivation normalized to the peak current (I_{P1}) at a recovery potential of −90 mV in the presence of different concentrations of extracellular potassium is shown for both channel types. (*D*) Time constants estimated from measurements as described in *C* are plotted against the extracellular potassium concentration $[K^+]_o$ ($n = 5$).

displayed a monoexponential time course for both channels (data not shown). The voltage dependence of recovery from inactivation was reduced for Kv2.1/Kv9.3. The two channels recovered equally fast at −130 mV but clearly diverged at more depolarized potentials, resulting in an approximately fourfold faster recovery rate at −80 mV for Kv2.1/Kv9.3 compared with Kv2.1 (Fig. 4 *B*; Table 1).

Extracellular potassium is known to influence recovery from most types of inactivation, including that of Kv2.1 (Demo and Yellen, 1991; Pardo et al., 1992; Baukrowitz and Yellen, 1995; Levy and Deutsch, 1996a,b; Klemic et al., 1998). Therefore, we tested the influence of different extracellular potassium concentrations (2.5, 50, 100 mM) on the recovery of Kv2.1/Kv9.3 and Kv2.1 (Fig. 4, *C* and *D*). The heteromeric channels did not show changes in the rate of recovery in the presence of increasing concentrations of extracellular potassium. In contrast, recovery from inactivation of Kv2.1 homomers was accelerated at elevated potassium concentrations, in agreement with findings of Klemic et al. (1998) (Fig. 4, *C* and *D*).

Cumulative inactivation increases with stimulation frequency for Kv2.1/Kv9.3

A number of potassium channels show cumulative inactivation, defined as a progressive decline in the amplitude of currents during a train of repetitive depolarizations. In this series of pulses the current amplitude at the beginning of a pulse is lower than at the end of the preceding one (Aldrich, 1981). Kv2.1/Kv9.3 showed both accelerated inactivation from the intermediate closed state (Fig. 3) and recovery from inactivation (Fig. 4). Consequently, one would predict the maximum of cumulative inactivation to be shifted toward higher frequencies. We compared the influence of repetitive pulsing (1, 4, and 8 Hz) between −90 mV and +40 mV on homomeric Kv2.1 (Fig. 5 *A*) and heteromeric Kv2.1/Kv9.3 (Fig. 5 *B*). For both channels, the normalized current (I_{Pn}/I_{P1}) was plotted against the time, and a monoexponential function was fitted to the data. At a stimulation frequency of 1 Hz, the current amplitude of Kv2.1 was decreased by 13%, and an equilibrium between inactivation and recovery was reached with a time constant of ~3.5 s, which was nearly identical to the measured time constant for inactivation from the open state (Fig. 2 *A*). Higher frequency of stimulation resulted in a slightly faster decrease of the relative current amplitudes, reaching the same equilibrium (Fig. 5 *A*). In comparison, Kv2.1/Kv9.3 showed a faster cumulative inactivation at all stimulation frequencies tested (Fig. 5 *B*). The time constant for reaching maximum cumulative inactivation at a stimulation frequency of 1 Hz was more than sixfold faster than the time constant measured for inactivation during a prolonged depolarization. Furthermore, cumulative inactivation increased with increasing stimulation frequencies (Fig. 5 *B*).

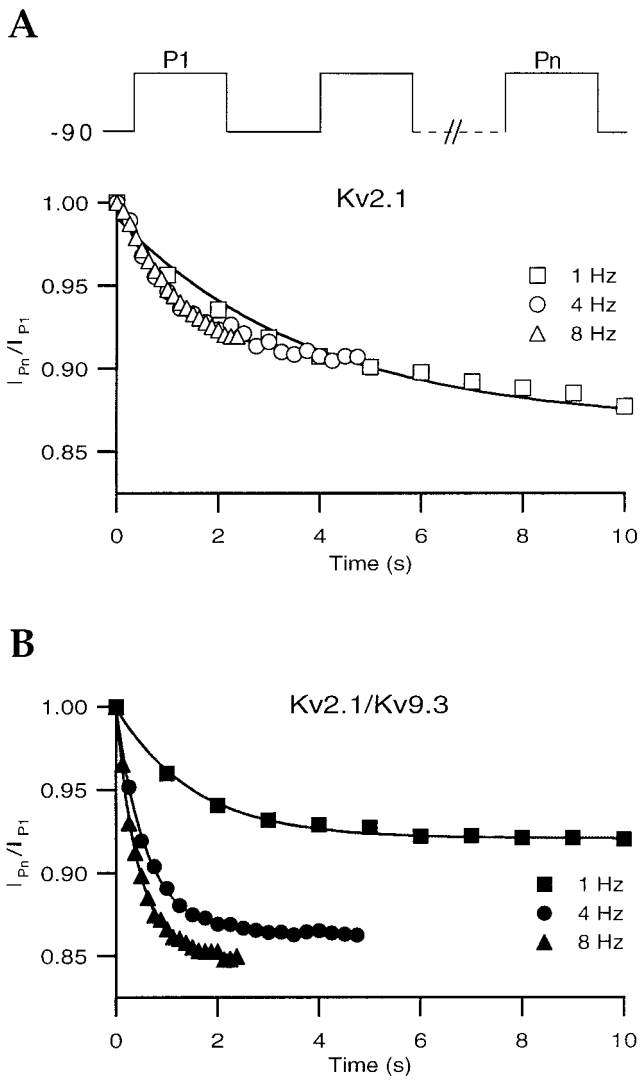

FIGURE 5 Kv2.1 and Kv2.1/Kv9.3 show different frequency dependence of cumulative inactivation. Cumulative inactivation was elicited by pulsing between −90 and +40 mV (P1), with equal time spent at both potentials. The frequencies of stimulation were 1, 4, and 8 Hz. Monoexponential functions were fitted to the decline of normalized current amplitudes Kv2.1 (*A*) ($n = 5$) and Kv2.1/Kv9.3 (*B*) ($n = 5$).

DISCUSSION

Composition of the characterized Kv2.1/Kv9.3 heteromer

Whereas injection of a mixture containing 10-fold more Kv9.3 than Kv2.1 cRNA into oocytes resulted in a complete suppression of Kv2.1 currents (Stocker et al. 1999), injection of only fivefold more Kv9.3 than Kv2.1 cRNA in this study led to the formation of conducting Kv2.1/Kv9.3 heteromers. Assuming a comparable translation of Kv2.1 and Kv9.3 cRNA and a random assembly of α-subunits, the probability of generating homomeric Kv2.1 channels with the cRNA ratio used in this study is lower than 0.2%. This view is supported by the fact that the inactivation of Kv2.1/Kv9.3 currents is complete at potentials where Kv2.1 alone

does not inactivate (−40 mV in Fig. 2 *C*). Assembly studies using the yeast two-hybrid system have shown that Kv9.3 α-subunits do not have the capability to interact in a homomeric fashion (Stocker et al., 1999). Therefore, the generated functional channels could only contain one, two, or three Kv9.3 α-subunits. Based on the specific down-regulation of Kv2.1 currents observed (Stocker et al., 1999), heteromers containing three Kv9.3 and one Kv2.1 subunit can be regarded as nonconducting. Finally, the half-maximum inhibitory concentration of tetraethylammonium for the Kv2.1/Kv9.3 heteromer was nearly identical to that measured for the Kv2.1 homomer (data not shown), arguing that mainly Kv2.1/Kv9.3 heteromers with only one Kv9.3 α-subunit underly the currents characterized in this paper.

Kinetic properties of Kv2.1/Kv9.3 compared to other Kv2.1/modulatory α-subunit heteromers

The increasing number of modulatory α-subunits recently cloned were all found to regulate biophysical, pharmacological, and metabolic properties of α-subunits belonging to the Kv2 subfamily (Post et al., 1996; Castellano et al., 1997; Patel et al., 1997; Salinas et al., 1997a,b; Kramer et al., 1998). In the following, we compare the different biophysical properties of Kv2.1 homomers and heteromers resulting from its coexpression with the mammalian modulatory α-subunits Kv5.1, Kv6.1, Kv8.1, and Kv9.1–3.

Similar to our observations, a slowing of current rise time has been reported for Kv2.1/Kv8.1 and Kv2.1/Kv5.1 (Castellano et al., 1997; Salinas et al., 1997a; Kramer et al., 1998). In contrast, coexpression of Kv9.1, Kv9.2, or Kv6.1 with Kv2.1 induced no or only minor changes in the time course of activation (Salinas et al., 1997b; Kramer et al., 1998). For Kv2.1/Kv9.3 (Patel et al., 1997; this work) and Kv2.1/Kv6.1 (Kramer et al., 1998), steady-state activation curves were shifted to hyperpolarized potentials in comparison with Kv2.1, whereas depolarized shifts were reported for Kv2.1/Kv8.1 and Kv2.1/Kv5.1 (Castellano et al., 1997; Salinas et al., 1997a; Kramer et al., 1998). In all studies so far, currents arising from coexpressions with modulatory α-subunits were found to deactivate severalfold more slowly than homomeric Kv2.1 channels (Post et al., 1996; Castellano et al., 1997; Salinas et al., 1997b; Kramer et al., 1998).

In this context it should be mentioned that in a previous publication coexpression of Kv2.1 and Kv9.3 in a ratio of 1:2 resulted in a current increase (Patel et al., 1997). The generated Kv2.1/Kv9.3 heteromers, in contrast to the results presented in this work, showed a monophasic and accelerated activation (Patel et al., 1997). Although qualitatively the displacement of the steady-state activation and inactivation curves and the deactivation behavior reported by Patel et al. (1997) are in agreement with the data presented in this work, the actual voltages for half-maximum activation and inactivation, as well as the time constants of deactivation, diverge quite substantially. This discrepancy might be explained in part by the use of a different ratio of Kv2.1 and Kv9.3 cRNAs.

In this comparative study of Kv2.1/Kv9.3 and Kv2.1 we mainly focused on inactivation and recovery from it. The corresponding results have been interpreted in view of a recent model proposed for inactivation of Kv2.1 that adapts the Monod-Wyman-Changeux model for allosteric proteins (Monod et al., 1965) to an ion channel (Klemic et al., 1998). In the proposed model, the four transitions between closed states preceding the opening transition are each accompanied by an exponential increase in the probability of inactivation. These transitions were assumed to be independent and kinetically identical. These assumptions are not valid in the case of a heteromeric channel with different subunits involved in its gating. Consequently, we proposed a simple, qualitative model (Fig. 3 *A*) useful for the interpretation of our data on inactivation.

We have shown that the inactivation of Kv2.1/Kv9.3 is a state-dependent process. Most Kv potassium channels either open before inactivation or inactivate from both open and closed states (Hille, 1992). In contrast, Kv2.1/Kv9.3 inactivates in a fast and complete manner from intermediate closed states, whereas inactivation from open conformations ($O \rightarrow I_o$) is inhibited. This explains its U-shaped steady-state inactivation curve, where inactivation is complete at voltages below the threshold of activation, and fewer channels inactivate during more depolarized conditioning pulses as they start to open. The residual inactivation that occurred during maintained depolarizations to +40 mV (Fig. 3 *A*) can be explained by channel closure occurring even at maximum open probability and allowing inactivation from C_i. The opposing regulation of Kv2.1's inactivation from closed versus open states by coexpression with Kv9.3 evidences that distinct molecular mechanisms account for these transitions. Investigations of inactivation properties of heteromeric channels resulting from the association of other modulatory α-subunits with Kv2.1 have produced a variety of results. Thus inactivation from open states was inhibited upon coexpression of Kv2.1 with Kv6.1 (Kramer et al., 1998), Kv8.1 (Castellano et al., 1997; Salinas et al., 1997a), and Kv9.3 (this work). Heteromeric Kv2.1/Kv5.1 channels display a more pronounced and Kv2.1/Kv6.1 a less pronounced inactivation from intermediate closed states (Kramer et al., 1998). There are no data available on closed state inactivation of heteromers involving Kv8.1, Kv9.1, and Kv9.2. Nonetheless, judging from the more obviously U-shaped steady-state inactivation curve of Kv2.1/Kv8.1 in comparison with that of Kv2.1 (Salinas et al., 1997a), it is likely that these channels also inactivate more completely from intermediate closed than from open states.

Possible physiological implications of Kv2.1/Kv9.3 characteristics

The observed changes in the gating of Kv2.1/Kv9.3 in comparison with the homomeric Kv2.1 suggest a distinct

role for the heteromer in the control of membrane potential and in the electrical signaling of cells. The shift of steady-state activation to hyperpolarized potentials suggests that Kv2.1/Kv9.3 contributes to the stabilization of the resting membrane potential.

The slow deactivation of Kv2.1/Kv9.3 prolongs current decay toward time scales (~100 ms) that fit a possible function of this channel in regulating the steepness of pacemaker depolarizations and consequently the frequency of repetitive firing of cells (McCormick, 1989; Irisawa et al., 1993). Consequently, Kv2.1/Kv9.3 might protect cells from premature excitations and their fatal consequences, as observed in some forms of cardiac arrhythmia. Furthermore, the fast inactivation from intermediate closed states of the Kv2.1/Kv9.3 heteromer has its maximum below the threshold for action potential generation. Therefore Kv2.1/Kv9.3 is primarily susceptible to inactivation in the ascent to threshold. The time spent on this process is significant whenever pacemaker depolarizations—as in some cells of heart (Irisawa et al., 1993), brain (Pape, 1996), and visceral smooth muscle (Kuriyama et al., 1998)—are the driving force toward threshold. The shorter this period, the higher the conductance available to repolarize the following action potential.

Inactivation of Kv2.1 and Kv2.1/Kv9.3 is a state-dependent process, which occurs for Kv2.1 from both the intermediate closed and the open state (Klemic et al., 1998), and for Kv2.1/Kv9.3 only from the intermediate closed state (C_i). Furthermore, for Kv2.1/Kv9.3 the time needed to reach C_i determines the rate of inactivation. This time depends on whether channels are depolarized from the resting potential ($C \rightarrow C_i$) or repolarized from depolarized potentials ($O \rightarrow C_i$), and as the time constants of the respective transitions have opposite voltage dependence, inactivation of this heteromeric channels senses the direction of a step that led to a given potential.

A role for modulatory α-subunits in the heart?

A target of prime interest for modulation of delayed rectifier currents is the shaping of cardiac action potentials (Barry and Nerbonne, 1996; Nerbonne, 1998). Kv9.3, like Kv2.1, displays high expression in this tissue (Drewe et al., 1992; Xu et al., 1996; Stocker and Kerschensteiner, 1998). Two questions are of central interest concerning the involvement of ion channels in mediating the electrical activity of heart cells. First, which channel subunits underlie the native currents in cardiomyocytes? Second, how do these currents determine the course of the action potential that governs the beating of the heart? For a number of voltage-dependent potassium currents in the rat heart, correlations to cloned Kv channels have been established (Barry and Nerbonne, 1996; Nerbonne, 1998), based on kinetic and pharmacological properties of Kv channels in conjunction with regional and developmental variations in their mRNA and protein distribution. In ventricular myocytes from adult rats, two components of delayed rectification have been described: I_{Kr}, mediated by eag-related gene (ERG) subunits (Nerbonne, 1998), and I_K (Apkon and Nerbonne, 1991). Among the Kv α-subunits known at the time to be expressed in the rat heart (Kv1.2, Kv1.4, Kv1.5, Kv2.1, Kv4.2), the closest resemblance to I_K was found for Kv2.1, which was consequently claimed to mediate this current. However, none of the criteria used to establish this correlation (Apkon and Nerbonne, 1991) readily differentiate between Kv2.1 homomers and heteromeric channels formed by its association with recently identified modulatory α-subunits. Moreover, mismatches between Kv2.1 and I_K (Xu et al., 1996) make the participation of additional subunits in the formation of channels underlying I_K a likely scenario. Interestingly, in addition to I_K, a delayed rectifier current that does not inactivate at depolarized potentials, similar to Kv2.1/Kv9.3 and unlike Kv2.1, was observed in 10% of ventricular cardiomyocytes (Apkon and Nerbonne, 1991). Thus it is tempting to speculate that Kv9.3 and other modulatory α-subunits participate in channels underlying the late repolarization and possibly regulating the steepness of diastolic depolarizations of rat ventricular cardiomyocytes. Nevertheless, definite understanding of the subunit composition of channels encoding I_K has to await biochemical identification.

We are grateful to Dr. Walter Stühmer for generous support and Drs. Walter Stühmer, Florentina Soto, and Paola Pedarzani for valuable scientific discussion and critical reading of the manuscript. We thank Susanne Voigt for *Xenopus* oocyte injections.

REFERENCES

Aldrich, R. W. 1981. Inactivation of voltage-gated delayed potassium current in molluscan neurons: a kinetic model. *Biophys. J.* 36:519–532.

Apkon, M., and J. M. Nerbonne. 1991. Characterization of two distinct depolarization-activated K^+ currents in isolated adult rat ventricular myocytes. *J. Gen. Physiol.* 97:973–1011.

Barry, D. M., and J. M. Nerbonne. 1996. Myocardial potassium channels: electrophysiological and molecular diversity. *Annu. Rev. Physiol.* 58: 363–394.

Barry, D. M., J. S. Trimmer, J. P. Merlie, and J. M. Nerbonne. 1995. Differential expression of voltage-gated K^+ channel subunits in adult rat heart. Relation to functional K^+ channels? *Circ. Res.* 77:361–369.

Baukrowitz, T., and G. Yellen. 1995. Modulation of K^+ current by frequency and external $[K^+]$: a tale of two inactivation mechanisms. *Neuron.* 15:951–960.

Castellano, A., M. D. Chiara, B. Mellstrom, A. Molina, F. Monje, J. R. Naranjo, and J. Lopez-Barneo. 1997. Identification and functional characterization of a K^+ channel α-subunit with regulatory properties specific to brain. *J. Neurosci.* 17:4652–4661.

Christie, M. J., R. A. North, P. B. Osborne, J. Douglass, and J. P. Adelman. 1990. Heteropolymeric potassium channels expressed in *Xenopus* oocytes from cloned subunits. *Neuron.* 2:405–411.

Demo, S. D., and G. Yellen. 1991. The inactivation gate of the Shaker K^+ channel behaves like an open-channel blocker. *Neuron.* 7:743–753.

Drewe, J. A., S. Verma, G. Frech, and R. H. Joho. 1992. Distinct spatial and temporal expression patterns of K^+ channel mRNAs from different subfamilies. *J. Neurosci.* 12:538–548.

Frech, G. C., A. M. J. VanDongen, G. Schuster, A. M. Brown, and R. H. Joho. 1989. A novel potassium channel with delayed rectifier properties isolated from rat brain by expression cloning. *Nature.* 340:642–645.

Hille, B. 1992. Ionic Channels of Excitable Membranes. Sinauer Associates, Sunderland, MA.

Hugnot, J. P., M. Salinas, F. Lesage, E. Guillemare, J. Deweille, C. Heurteaux, M. G. Mattei, and M. Lazdunski. 1996. Kv8.1, a new neuronal potassium channel subunit with specific inhibitory properties towards Shab and Shaw channels. *EMBO J.* 15:3322–3331.

Hwang, P. M., C. E. Glatt, D. S. Bredt, G. Yellen, and S. H. Snyder. 1992. A novel K^+ channel with unique localizations in mammalian brain: molecular cloning and characterization. *Neuron.* 8:473–481.

Irisawa, H., H. F. Brown, and W. Giles. 1993. Cardiac pacemaking in the sinoatrial node. *Physiol. Rev.* 73:197–227.

Isacoff, E. Y., Y. N. Jan, and L. Y. Jan. 1990. Evidence for the formation of heteromultimeric potassium channels in *Xenopus* oocytes. *Nature.* 345:530–534.

Klemic, K. G., C. C. Shieh, G. E. Kirsch, and S. W. Jones. 1998. Inactivation of Kv2.1 potassium channels. *Biophys. J.* 74:1779–1789.

Kramer, J. W., M. A. Post, A. M. Brown, and G. E. Kirsch. 1998. Modulation of potassium channel gating by coexpression of Kv2.1 with regulatory Kv5.1 or Kv6.1 α-subunits. *Am. J. Physiol.* 274: C1501–C1510.

Krieg, P. A., and D. A. Melton. 1987. In vitro RNA synthesis with SP6 RNA polymerase. *Methods Enzymol.* 155:397–415.

Kuriyama, H., K. Kitamura, T. Itoh, and R. Inoue. 1998. Physiological features of visceral smooth muscle cells, with special reference to receptors and ion channels. *Physiol. Rev.* 78:811–920.

Levy, D. I., and C. Deutsch. 1996a. Recovery from C-type inactivation is modulated by extracellular potassium. *Biophys. J.* 70:798–805.

Levy, D. I., and C. Deutsch. 1996b. A voltage-dependent role for K^+ in recovery from C-type inactivation. *Biophys. J.* 71:3157–3166.

MacKinnon, R. 1991. Determination of the subunit stoichiometry of a voltage-activated potassium channel. *Nature.* 350:232–235.

McCormick, D. A. 1989. Cholinergic and noradrenergic modulation of thalamocortical processing. *Trends Neurosci.* 12:215–221.

Monod, J., J. Wyman, and J.-P. Changeux. 1965. On the nature of allosteric transitions: a plausible model. *J. Mol. Biol.* 12:88–118.

Nerbonne, J. M. 1998. Regulation of voltage-gated K^+ channel expression in the developing mammalian myocardium. *J. Neurobiol.* 37:37–59.

Pape, H. C. 1996. Queer current and pacemaker: the hyperpolarization-activated cation current in neurons. *Annu. Rev. Physiol.* 58:299–327.

Parcej, D. N., V. E. S. Scott, and J. O. Dolly. 1992. Oligomeric properties of a-dendrotoxin-sensitive potassium ion channels purified from bovine brain. *Biochemistry.* 11084–11088.

Pardo, L. A., S. A. Heinemann, H. Terlau, U. Ludewig, C. Lorra, O. Pongs, and W. Stühmer. 1992. Extracellular K^+ specifically modulates a rat brain K^+ channel. *Proc. Natl. Acad. Sci. USA.* 89:2466–2470.

Patel, A. J., M. Lazdunski, and E. Honore. 1997. Kv2.1/Kv9.3, a novel ATP-dependent delayed-rectifier K^+ channel in oxygen-sensitive pulmonary artery myocytes. *EMBO J.* 16:6615–6625.

Post, M. A., G. E. Kirsch, and A. M. Brown. 1996. Kv2.1 and electrically silent Kv6.1 potassium channel subunits combine and express a novel current. *FEBS Lett.* 399:177–182.

Quattrocki, E. A., J. Marshall, and L. K. Kaczmarek. 1994. A Shab potassium channel contributes to action potential broadening in peptidergic neurons. *Neuron.* 12:73–86.

Rettig, J., S. H. Heinemann, F. Wunder, C. Lorra, D. N. Parcej, J. O. Dolly, and O. Pongs. 1994. Inactivation properties of voltage-gated K^+ channels altered by presence of β-subunit. *Nature.* 369:289–294.

Ruppersberg, J. P., K. H. Schroter, B. Sakmann, M. Stocker, S. Sewing, and O. Pongs. 1990. Heteromultimeric channels formed by rat brain potassium-channel proteins. *Nature.* 345:535–537.

Salinas, M., J. Deweille, E. Guillemare, M. Lazdunski, and J. P. Hugnot. 1997a. Modes of regulation of Shab K^+ channel activity by the Kv8.1 subunit. *J. Biol. Chem.* 272:8774–8780.

Salinas, M., F. Duprat, C. Heurteaux, J. P. Hugnot, and M. Lazdunski. 1997b. New modulatory alpha subunits for mammalian Shab K^+ channels. *J. Biol. Chem.* 272:24371–24379.

Stocker, M., M. Hellwig, and D. Kerschensteiner. 1999. Subunit assembly and domain analysis of electrically silent K^+ channel α-subunits of the rat Kv9 subfamily. *J. Neurochem.* 72:1725–1734.

Stocker, M., and D. Kerschensteiner. 1998. Cloning and tissue distribution of two new potassium channels α-subunits from rat brain. *Biochem. Biophys. Res. Commun.* 248:927–934.

Stühmer, W. 1992. Electrophysiological recordings from *Xenopus* oocytes. *Methods Enzymol.* 207:319–339.

Tsunoda, S., and L. Salkoff. 1995. The major delayed rectifier in both Drosophila neurons and muscle is encoded by Shab. *J. Neurosci.* 15: 5209–5221.

Van Dongen, A. M. J., G. C. Frech, J. A. Drewe, R. H. Joho, and A. M. Brown. 1990. Alteration and restoration of K channel function by deletions at the N- and C-termini. *Neuron.* 5:433–443.

Xu, H., J. E. Dixon, D. M. Barry, J. S. Trimmer, J. P. Merlie, D. McKinnon, and J. M. Nerbonne. 1996. Developmental analysis reveals mismatches in the expression of K^+ channel alpha subunits and voltage-gated K^+ channel currents in rat ventricular myocytes. *J. Gen. Physiol.* 108:405–419.